Original Article

JCBFM

Journal of Cerebral Blood Flow & Metabolism
2018, Vol. 38(5) 888–903
© Author(s) 2017
Reprints and permissions:
sagepub.co.uk/journalsPermissions.nav
DOI: 10.1177/0271678X17708690
journals.sagepub.com/home/jcbfm
SAGE

Characterization of human fetal brain endothelial cells reveals barrier properties suitable for in vitro modeling of the BBB with syngenic co-cultures

Allison M Andrews[1,2], Evan M Lutton[1], Lee A Cannella[1,2], Nancy Reichenbach[1], Roshanak Razmpour[1], Matthew J Seasock[1], Steven J Kaspin[1], Steven F Merkel[1,2], Dianne Langford[3], Yuri Persidsky[1,2] and Servio H Ramirez[1,2,4]

Abstract

Endothelial cells (ECs) form the basis of the blood–brain barrier (BBB), a physical barrier that selectively restricts transport into the brain. In vitro models can provide significant insight into BBB physiology, mechanisms of human disease pathology, toxicology, and drug delivery. Given the limited availability of primary human adult brain microvascular ECs (*aBMVECs*), human fetal tissue offers a plausible alternative source for multiple donors and the opportunity to build syngenic tri-cultures from the same host. Previous efforts to culture fetal brain microvascular ECs (*fBMVECs*) have not been successful in establishing mature barrier properties. Using optimal gestational age for isolation and flow cytometry cell sorting, we show for the first time that *fBMVECs* demonstrate mature barrier properties. *fBMVECs* exhibited similar functional phenotypes when compared to *aBMVECs* for barrier integrity, endothelial activation, and gene/protein expression of tight junction proteins and transporters. Importantly, we show that tissue used to culture *fBMVECs* can also be used to generate a syngenic co-culture, creating a microfluidic BBB on a chip. The findings presented provide a means to overcome previous challenges that limited successful barrier formation by *fBMVECs*. Furthermore, the source is advantageous for autologous reconstitution of the neurovascular unit for next generation *in vitro* BBB modeling.

Keywords

Blood–brain barrier, syngenic, BBB model, human fetal brain endothelial cells

Received 15 July 2016; Revised 28 March 2017; Accepted 30 March 2017

Introduction

During development, endothelial cells (ECs) arise from a common precursor and then differentiate in response to the local environment and interactions with surrounding cells in order to perform tissue specific functions.[1] Cerebral vasculature in particular is highly specialized compared to vessels in other tissues. Brain endothelium lacks fenestrations, exhibits low level endocytotsis and plasma membrane invaginations (i.e. clatherin-coated pits, caveolae),[2] is highly polarized, and differentially distributes proteins and transporters to apical versus basolateral surfaces in order to support diverse functions of the blood–brain barrier (BBB).[3] In addition, neighboring brain ECs express unique tight junction (TJ) complexes, forming

[1]Department of Pathology & Laboratory Medicine, Lewis Katz School of Medicine, Temple University, Philadelphia, PA, USA
[2]The Center for Substance Abuse Research, Lewis Katz School of Medicine, Temple University, Philadelphia, PA, USA
[3]Department of Neuroscience, Lewis Katz School of Medicine, Temple University, Philadelphia, PA, USA
[4]The Shriners Hospitals Pediatric Research Center, Philadelphia, PA, USA

Corresponding author:
Servio H Ramirez, Pathology and Laboratory Medicine, Lewis Katz School of Medicine at Temple University, 3500 N Broad St, Philadelphia, PA 19140, USA.
Email: servio.ramirez@temple.edu

a vascular tunic that manifests ''barrier'' properties regulating the exchange of molecules between the blood and brain parenchyma. Several studies have reported that during BBB development, a transition occurs from an immature barrier to a more mature barrier which correlates with changes in TJ localization (immunofluorescence or freeze fracture) in the human fetus[4–6] and rat.[7] It is hypothesized that this transition explains the decreased vessel fragility in the germinal matrix at later gestational ages.[5,6,8] The formation of TJs mark the beginning of mature BBB development, and Virgintino et al.[4] showed that in the human fetus, which occurs around 14 weeks of gestation. Ballabh et al.[6] and Anstrom et al.[5] have also shown mature staining of TJPs in the cortex as early as 16 weeks, although they reported differences in the time of maturity development in the germinal matrix. Additionally, Licht et al.[8] have proposed that cortical vessel maturity is progressive and wave-like where periventricular vessels in the germinal matrix mature last. The formation of TJ complexes occurs due to cytoskeletal rearrangements that promote re-localization of tight junction proteins (TJPs), specifically occludin and claudin-5, which shift from cytoplasmic to membranous expression.[4] Considering these data, *f*BMVECs isolated post-barrier development (i.e. greater than gestational week 14) will likely retain much of the barrier phenotype and protein expression known to support BBB function in vivo, and may therefore be suitable for in vitro modeling.

While significant advancements in understanding BBB physiology and function have been made since the development of protocols to culture brain ECs from laboratory animals,[9,10] the field still encounters tremendous challenges in translating results obtained from animal-derived cultures to humans. This deficit in animal modeling is particularly important when assessing drug pharmacodynamics. For example, previous studies have shown that the expression of Pgp and BCRP-1 differs between species, or non-EC cell lines and human brain ECs.[11] Also, pathophysiology and drug targeting discovery are hindered by protein expression distinctions and divergence in signaling mechanisms between species. Although immortalized human brain ECs are commonly used (such as the hCMEC/D3 line), concerns over lack of contact inhibition, chromosomal rearrangement and aberrations limits their utility.[12] Like few other labs worldwide, we routinely isolate and expand cell cultures of brain ECs derived from healthy resection paths from patients undergoing temporal lobe resective surgery for epilepsy. However, due to the invasiveness nature of the procedure, gamma knife radiosurgery is becoming favored in intractable epilepsy[13] and will begin to affect this tissue availability for use in research. Thus, *fBMVEC*s could offer an alternative source of brain ECs. Previous problems associated with culturing *fBMVEC*s included minimal barrier maturity and high glial and pericyte presence. A single recent report can be found that showed methodology for isolation of human fetal ECs.[14] Although the expansion of ECs in the report above was shown, it is unclear whether their preparation would yield mature brain ECs for BBB modeling given that vessels were isolated early in the first trimester and no functional assays were provided.[14] In this report, we have outlined that it is essential to use fetal vessels after 14 weeks for isolation of brain ECs and that strategic serial cell sorting by flow cytometry minimizes astrocyte and pericyte takeover.

Importantly, we provide in this report a comparative analysis of barrier properties between *fBMVEC*s and *aBMVEC*s, evidence for the functional presence of barrier formation in monolayers of *fBMVEC*s and lastly, that *fBMVEC*s allows for the advantage to generate syngenic co- or tri-cultures with astrocytes and pericytes in in vitro microfluidic BBB models. Overall, the use of primary human *fBMVEC*s in co-culture with members of the neurovascular unit in microfluidic chips could usher in the next generation of improved BBB models for assaying CNS toxicology, CNS drug penetration, drug delivery and understanding BBB damage during various neuropathologies.

Materials and methods

Reagents

Dexamethasone was purchased from Sigma (St. Louis, MO, USA). Recombinant human TNF-α was purchased from R&D Systems (Minneapolis, MN, USA). Rat-tail collagen I and endothelial cell growth supplement (ECGS) were purchased from BD Biosciences (Franklin Lakes, NJ, USA). Heparin, DMEM/Ham's F12 media, Fetal bovine serum (FBS) were purchased from Thermo Fisher Scientific (Waltham, MA, USA).

Tissue preparation

Healthy tissue from fetal brains collected (under informed consent) by the Laboratory of Developmental Biology (University of Washington, Seattle, WA) or via the Temple University's Comprehensive NeuroAIDS Center were used with approval granted by Temple University's (Philadelphia, PA) Institutional Review Board and in full compliance by the National Institutes of Health's (NIH) ethical guidelines. Brain tissue was washed in 2–3× in Hank's Balanced Salt Solution (HBSS) and pelleted at 1000 r/min for 5 min. Tissue was

then processed for microvessel isolation and staining (see below) or EC isolation and culture (see section below on *Human fetal brain endothelial cell isolation and cell culture*).

Microvessel immunofluorescence staining

The obtained brain tissue was diced using sterile blades then homogenized in 1 ml 1 × HBSS using a Dounce manual homogenizer. The resulting suspension was centrifuged at 1000 × *g* for 10 min and the supernatant discarded. The pellet was resuspended in 5 ml 17.5% dextran (MW: 86,000, MP Biomedicals, LLC) in HBSS. Microvessels were pelleted by centrifugation at 4400 × *g* for 15 min. The pelleted contents were resuspended in 5 ml 1% BSA in HBSS. Using a 5 ml serological pipet, the suspension was disrupted by pipetting up and down against a cell culture dish 10 times. The suspension was passed through a 40 μm cell strainer (Falcon) to capture the microvessels. The strainer was inverted and rinsed into a clean cell culture dish with a total volume of 3 ml 1% BSA in HBSS. Microvessels were removed from suspension by centrifugation at 10,000 × *g* for 10 min. Microvessels were resuspended in PBS, plated on Poly-L-Lysine-coated coverslips, and allowed to attach with incubation for 1 h at 37°C. Vessels were fixed using 3% formaldehyde in PBS for 10 min at RT and then permeabilized using 0.1% Triton X-100 in PBS for 5 min at RT. Following permeabilization, non-specific binding sites were blocked using 5% BSA in PBS for 30 min at RT. The following antibodies were diluted at the respective ratios in 5% BSA in PBS and incubated overnight at 4°C: Occludin 1:50 (Santa Cruz sc-8145), platelet endothelial cell adhesion molecule-1 (PECAM-1) 1:50 (Santa Cruz sc-1506), glucose transporter-1 (Glut-1) 1:80 (abcam ab40084), Tricellulin 1:1000 (Millipore AB2980), and zona occludens-1 (ZO-1) 1:100 (Invitrogen 402300). Vessels were washed and incubated with corresponding Alexa Fluor secondary antibodies (1:200) in the dark for 1 h at RT followed by a 30 min stain with DAPI. Microvessels were imaged by confocal microscopy. Pseudocolor and line intensity analysis were performed using Imaris 8.2 (Bitplane) software. MeasurementPro module (Imaris) was utilized to measure line intensity at vessel borders. Measurements were obtained across 10μm with a minimum of six measurements per vessel. Three vessels per stain per age were analyzed. Data are presented at mean ± S.E.M.

Human fetal brain endothelial cell isolation and cell culture

To isolate endothelial cells, first the tissue (1–5 cm^3) was digested in 0.5% collagenase in PBS at 37°C for 40 min. Following digestion, the tissue suspension was washed with HBSS, centrifuged at 1000 r/min for 5 min and the supernatant discarded. The pellet was resuspended in 12 ml sterile 17.5% dextran (MW 86,000, MP Biomedicals, LLC) in HBSS. Vessels were pelleted by centrifugation at 4400 × *g* for 15 min. Vessels were isolated from the wall of the centrifuge tube and passed through sequential filters (100 μm and 40 μm, Falcon). Vessels caught in the 40 μm filter were then plated onto human fibronectin (Thermo Fisher Scientific)-coated T-25 cm^2 flasks. For experimental conditions, the cells were cultured in our "endothelial growth media" (see the following section on *Adult microvascular endothelial cell culture*) until confluency.[15] *fBMVEC*s were further purified using flow cytometry to remove contaminating astrocytes or pericytes. For cell sorting, *fBMVEC*s were trypsinized and washed using BD pre-sort buffer (BD Biosciences) and labeled using intercellular adhesion molecule (ICAM-1) (PE, Affirmetrix) and platelet-derived growth factor receptor beta (PDGFRβ) (APC, Affirmetrix). Cells were passed through a 40 μm filter to disrupt cell clumps and obtain a single cell solution. *fBMVEC*s were sorted by gating for ICAM-1^+/PDGFRβ^- populations. *fBMVEC*s were plated onto collagen I-coated T-75 cm^2 flasks and during the first passage after sorting, cells were passed through a 40 μm strainer after trypsination prior to pelleting and resuspension.

Adult microvascular endothelial cell culture

Primary adult human brain microvascular endothelial cells (*aBMVEC*s), isolated from vessels from brain resection tissue (showing no abnormalities) of patients undergoing surgery for treatment of intractable epilepsy, were supplied by Michael Bernas and Dr. Marlys Witte (University of Arizona, Tucson, AZ, USA) and maintained as described.[15] All cells were grown in incubators set at 37°C and 5% CO_2. Both human fetal and adult brain endothelial cells were maintained in endothelial growth media containing 1 mg/ml Heparin (Sigma), 10% FBS (Gibco), 0.1 mg/ml ECGS (BD Biosciences), 100U/mL Penicillin/100 μg/ml Streptomycin (Life Technologies), and 2.5 μg/ml amphotericin B (Gibco) in DMEM/Ham's F12 media (Gibco). Low growth factor media consisted of 10% FBS with Penn/Strep and amphotericin B.

Trans-endothelial electrical resistance measurements

Isolated *fBMVEC*s and *aBMVEC*s were plated (20,000/well) on collagen I-coated 96-well electrode arrays (96W20idf, Applied Biophysics, Troy, NY, USA) and grown until confluent. Trans-endothelial electrical resistance (TEER) was measured every 1000 s at

4000 Hz using the electrical cell-substrate impedance sensing (ECIS) system (Applied Biophysics, Troy, NY, USA) as described previously.[16,17] Cells were grown until a constant baseline resistance was obtained and then media was replaced with low growth factor media. Cells were treated with 100 ng/mL of IL-1β, or 5 μM dexamethasone dissolved in low growth factor media and resistance was measured for 12 h. Results represent three to five replicates from each cell type or donor.

Flow cytometry analysis of cell adhesion molecule expression

Cells were washed with calcium and magnesium-free PBS. Cells were then trypsinized and pelleted by centrifugation at 1000 r/min for 5 min. Cells were re-suspended in fixation buffer (affirmetrix) and incubated for 10 min. Following fixation with 4% paraformaldehyde (affirmetrix), cells were washed with flow cytometry buffer (affirmetrix) and pelleted again. Cells were resuspended in 100 μl of flow cytometry buffer and anti-ICAM-1 (PE) preconjugated primary antibodies for 40 min. Cells were then washed, pelleted, and resuspended in flow cytometry buffer for flow cytometric analysis. A total of 10,000 events for each sample were acquired with an FACS BD Canto II flow cytometer (BD Biosciences) and analyzed with FlowJo software (Tree Star, Ashland, OR, USA).

Real-time qPCR

Total RNA from three biological replicates was isolated from BMVEC cultures for each donor using the RNeasy Mini Kit (QIAGEN) according to the manufacturer's instructions. RNA purity and concentration were determined using a NanoDrop ND-1000 spectrophotometer (Thermo Fisher Scientific, Fair Lawn, NJ). RNA was reverse transcribed using the High-Capacity cDNA Reverse Transcription Kit (Applied Biosystems, Foster City, CA). All Taqman probes were purchased from Life Technologies with the following catalog numbers: Occludin (hs00170162_m1), ZO-1/TJP1 (Hs0155 1861_m1), Claudin-5 (Hs00533949_s1), ABCG2/BCRP-1 (Hs01053790_m1), ABCB1/MDR-1 (Hs01067802_m1), SLC2A1/Glut-1 (Hs00892681_m1), ABCC1/MRP-1 (Hs00219905_m1), ABCC5/MRP-5 (Hs00981087_m1), PECAM (hs00169777_m1); Housekeeping genes: RPLPO (4333761F), 18 S (4310893F). Amplification was analyzed using the ΔΔCt method, using a web-based data analysis tool (SABiosciences, QIAGEN Inc., Valencia, CA, USA), by normalization to housekeeping genes. mRNA expression of the analyzed genes was reported for five adult and five fetal donors showing threshold cycles (ΔCT) ± standard error of the mean.

Monocyte adhesion assay

Monocytes were obtained from the University of Nebraska Medical Center in Omaha, NE. Cells were isolated from peripheral blood of hepatitis B seronegative, human donors by leukapheresis, and further purification by countercurrent centrifugal elutriation. Monocytes were used within 24 h of isolation. The Temple University Institutional Review Board approved all procedures involving the use of human monocytes in the following experiments. Monocyte adhesion assays were performed as previously described.[18] *fBMVE C*s were plated on 96-well plates (at a density of 2.5×10^4 *fBMVEC*/well). Briefly, monocytes were fluorescently labeled (2.5×10^5 cells/ml loaded with 5 μM Calcein-AM, Life Technologies, for 45 min). After stimulation with or without recombinant human tumor necrosis factor-α (TNF-α, R&D Systems, 20 ng/ml, 4 h), the endothelial cells were rinsed and fluorescently labeled monocytes (1×10^5 cells/well) were added to the EC monolayers for 15 min at 37°C. After adhesion, monolayers were washed and relative fluorescence of the attached monocytes was acquired on a fluorescence plate reader (Synergy 2, BioTek Instruments, Winooski, VT). Results are shown as fold difference in adherent monocytes normalized to the control condition.

Monocyte migration assay

Transendothelial migration assays were performed as previously described.[18] *fBMVEC*s were plated on collagen type I-coated FluoroBlok tinted tissue culture plates (3 μm pores, BD Biosciences, Franklin Lakes, NJ) at a density of 2.5×10^4 BMVEC/insert one week prior to use for migration assay. Medium was replaced, cell monolayers were washed, and monocyte chemotactic protein type 1 (MCP-1/CCL2, 30 ng/ml, R&D Systems) was added to the lower chamber. Monocytes were labeled with Calcein-AM as described for adhesion assays, washed, placed in the upper chamber, and allowed to migrate for 2 h at 37°C. The number of migrated monocytes was determined with ImageJ software, version 1.43 (NIH, Bethesda, MD) and is expressed for each experimental condition as the mean of triplicate. Data are presented as fold difference in migrated monocytes normalized by the control condition.

Western blot

Samples were lysed in Cell Lytic MT Cell Lysis Reagent (Sigma), sonicated for 3 s, and then centrifuged at $10{,}000 \times g$ for 15 min. Pellet was discarded and protein quantification was performed using the Pierce™ BCA

kit (Pierce/Thermo Fisher). Samples were mixed with 4 × lamelli buffer and boiled for 10 min. Samples were loaded onto a 4–20% Mini-Protean TGX gel (Biorad). Gels were transferred to nitrocellulose membranes using the Trans-Blot Turbo™ transfer system (Biorad) following the manufacturers protocol. Membranes were blocked with SuperBlock (Thermo Fisher) and all primary (1:1000) and secondary (1:10,000) antibodies were dissolved in SuperBlock (Thermo Fisher). Bound antibodies were exposed to Supersignal West Pico chemiluminescent substrate (Thermo Fisher).

Signal visualization was obtained using the gel documentation system, G:Box Chemi HR16 (Syngene, Frederick, MD).

Tri-culture microfluidic chips. *fBMVEC*s were plated onto collagen I coated outer "endothelial" channels of idealized co-culture microfluidic chips (SynVivo®, LLC) and grown until confluence. Astrocyte/pericyte cultures were trypsinized and labeled with Calcein-AM as described for adhesion assays. Labeled astrocytes/pericytes were then plated into the inner "CNS" compartment of the microfluidic chips and grown overnight. Fluorescently labeled tracers (sodium fluorescein, NaFluo Sigma Aldrich, and dextrans MW 3 and 40 kDa, Life Technologies) was dissolved in media and perfused in the outer endothelial compartment. Images were taken using an inverted live cell-imaging microscope (Zeiss Axiovert and HRM camera) with 10× and 20× microscope objectives.

Fluidic flow

*fBMVEC*s were plated onto collagen I-coated microfluidic channels (μ-Slide I 0.4 Luer, Ibidi USA, Inc., Madison, WI) and grown overnight. Low shear stress (1.5 dyn/cm^2) was applied using the Ibidi perfusion system for 12–24 h and then increased step wise until 10 dyn/cm^2 was reached. Cells were exposed to shear stress for an average of five days. Experiments were performed on three to four fetal donors. Images were taken using an inverted live cell-imaging microscope (Zeiss Axiovert and HRM camera).

Permeability

A mixture of fluorescence tracers (Sodium Fluorecein, abbreviated NaFluo, 3 kDa cascade blue, abbreviated CB dextranm and 40 kDa tetramethyrhodamine, abbreviated TMR dextran) was resuspended in low growth factor media and perfused in the endothelial compartment. Fluorescent images were captured using an inverted live cell-imaging microscope (Zeiss Axiovert and HRM camera) every 5 min for 30 min similarly to another study using the Synvivo® microfluidic chips.[19] Permeability was calculated using the following simplified equation based on the manufacturers instructions $P = \frac{1}{I_{vo}} \frac{V}{S} \frac{dI_t}{dt}$, where P is the apparent permeability in cm/s, I_{vo} is the intensity in the outer endothelial compartment, V/S is the ratio of volume to surface area of the outer endothelial compartment which is 0.1 cm, dI/dt is the change in basolateral intensity of time. dI/dt is calculated by plotting the intensity vs. time and fitting a line, where the slope is equal to dI/dt. Apparent permeability was calculated for three independent experiments. For experiments with LPS, following initial baseline measurements, channels were flushed with media and tracers mixed with 200 ng/ml of LPS and fluorescent images were acquired as above.

Statistical analysis

All experiments were performed on three or more fetal and adult donors. Data are expressed as the mean ± SEM. of experiments. Student's t-test with $^*p < 0.05$ was used to compare *fBMVEC*s and *aBMVEC*s results for significance. Statistical analyses were performed utilizing Prism v6.0 c software (GraphPad Software, San Diego, CA).

Results

TJP expression in fetal vessels is characteristic of mature barrier properties

With the growing demand for human brain ECs for therapeutic testing and BBB modeling, there is a great need for alternatives to the currently available sources. Fetal tissue represents a potential alternative, which is more readily available than adult tissue from deceased or epileptic patients.[15] However, due to the timeline for fetal brain development, it is necessary for the BBB to be fully formed and functional in order to obtain *fBMVEC*s that are suitable for study. In order to confirm the formation of a mature BBB, we isolated fetal brain microvessels and immunostained for TJPs and endothelial markers (Figure 1). Previous reports have shown that during development the most critical change in endothelial TJP expression in the brain (specifically with regards to occludin and claudin-5) occurs between 12 and 14 weeks of gestation.[4] This transitional phase culminates in the discrete expression of TJPs at cell–cell borders, which is considered a hallmark of mature TJ complexes and the formation of a functional physical BBB.[4,20]

Representative images for each immunostain are shown with arrowheads pointing to classic TJP localization and intercellular pattern. As expected, TJPs (occludin, ZO-1, claudin-5 and tricellulin) all exhibited the characteristic continuous and high expression

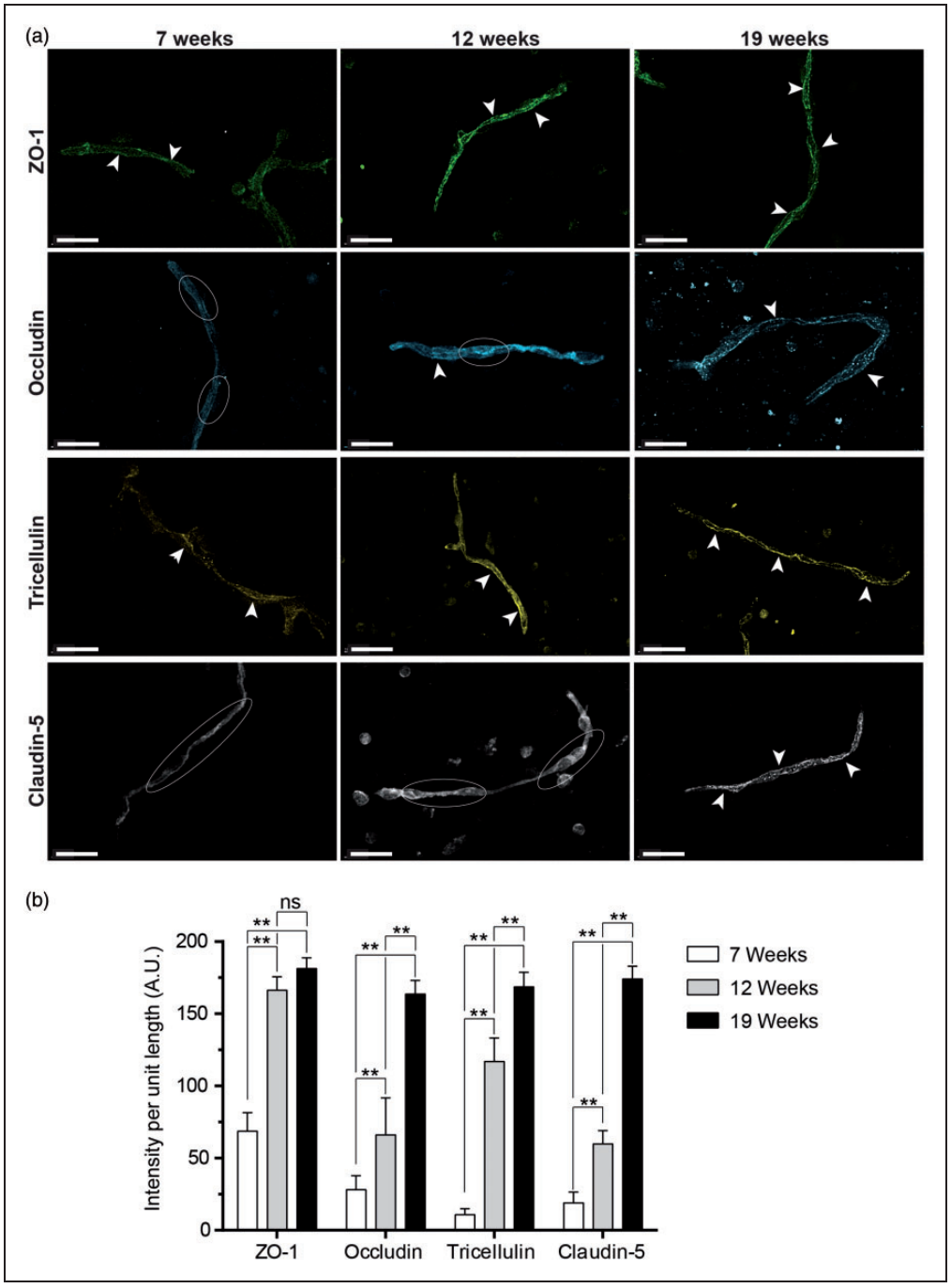

Figure 1. Immunofluorescence staining of protein localization in primary human fetal brain microvessels. Human fetal brain microvessels aged 7 weeks, 12 weeks, and 19 weeks were stained for tight junction proteins. Vessels were imaged using confocal microscopy. (a) Immunofluorescence staining of primary human fetal brain microvessels (7 and 12 weeks) showing continuous expression pattern of ZO-1 (green) and tricellulin (yellow), while occludin (Cyan) and claudin-5 (white) show an intracellular diffuse expression pattern. In contrast, vessels isolated post-barrier development (19 weeks) demonstrate continuous expression of tight junction proteins at the cell borders for occludin (Cyan), ZO-1 (green), claudin-5 (white) and Tricellulin (yellow). White arrows indicate continuous TJP expression while white ellipses highlight diffuse intracellular staining. Scale bar at 20 μm. (b) Bar graph quantification of line intensity profiles obtained using MeasurementPro (Imaris, Bitplane) for vessels of similar caliber (<15 μm diameter) for each of the gestational ages (Avg ± SEM).

pattern at the cell borders for vessels isolated at 19 weeks (Figure 1). Furthermore, the expression of key brain endothelial markers PECAM-1 and GLUT-1 was also high but mostly diffuse and throughout the vessel (data not shown) as expected. Following quantification of staining intensity at vessel borders (Figure 1(b)), TJP expression in fetal vessels was observed to change over time, which is reflected in images shown in Figure 1. Across gestational ages, all TJPs exhibited an increase in line intensity with increased age with the exception of ZO-1 for which line intensity was not significantly different between 12 and 19 weeks (Figure 1(b)). Overall, the elevated presence of TJPs, which form a continuous pattern at cell–cell borders and positive staining of endothelial markers, confirms that fetal cerebral endothelium at this stage in development express key essential components needed for proper barrier formation. Of note, vessels isolated earlier than 14 weeks have morphologically different patterns of TJP expression than those described above, with occludin and claudin-5 appearing diffuse and less intensely marginal (Figure 1).

Human fetal brain endothelial cell isolation and cell culture

Fetal brain tissue (16–22 weeks) was digested by collagenase I (to separate pericytes and astrocytes from the vessel) followed by dextran (17.5%) centrifugation (supplemental Figure 1(a)) to isolate microvessels. Sequential filtration through cell strainers removed excess remaining tissue and separated remaining intact microvessels from single cells. These vessels were then plated in cell culture flasks coated with human fibronectin and maintained in endothelial growth media for the expansion of primary human fetal brain microvascular endothelial cell (*f*BMVEC) cultures.

Isolated *f*BMVECs began as small colonies that grew outward radially. Cultures reached confluence within one to two weeks and exhibited typical endothelial cobblestone morphology when visualized with brightfield microscopy (supplemental Figure 1(b) and (d)). Additionally, this morphology was comparable to that of *a*BMVECs (data not shown).

In order to increase the purity of the *f*BMVEC cultures, the cells were sorted for ICAM-1 positive/PDGFR-β negative. Cells were then stained before and after sorting in order to determine the approximate astrocyte and pericyte content. Immunostaining prior to sorting showed ~5% presence of astrocytes and pericytes which could be significantly reduced to < 1% (supplemental Figure 2). Cells were further immunostained for key EC proteins to demonstrate phenotypical endothelial protein expression profiles and endothelial purity. Specifically, all cells were positive for endothelial marker Von Willibrand factor (VWF) (supplemental Figure 3), and TJP ZO-1 was clear and distinctly localized only at the cell borders (Figure 3(c)).

Comparative gene and protein expression analysis of ABC transporters and TJP between fBMVECs and aBMVECs

During development, the expression of TJs signifies the beginning of the formation of a mature BBB.[4] Furthermore, the detection of an intact transporter system is a hallmark of barrier maturation.[21] Therefore, in addition to the expression of TJPs (occludin, ZO-1, claudin-5), characterization of mRNA expression for transporters (BCRP-1, MRP-1, MRP-5, PGP-1, and GLUT-1) and the endothelial marker PECAM-1 in isolated *fBMVEC*s was performed. Expression levels were compared to *aBMVEC*s. After RNA isolation and cDNA conversion, the results of the quantitative PCR assay revealed that average ΔCT values for TJPs, occludin and ZO-1, and transporter genes, specifically BCRP-1, MRP-1, MRP-5, and PGP-1 were not significantly different between fetal and adult donors (Figure 2). Additionally, fetal donors expressed slightly lower levels of claudin-5 and Glut-1 and higher levels of PECAM-1. These results further support the notion that *fBMVEC*s isolated after 14 weeks have acquired barrier properties consistent with a mature BBB. This gene expression profile reflects the signature phenotype of enriched factors expressed at the BBB suggesting that *fBMVEC*s can be an alternate source of brain ECs suitable for modeling the BBB in vitro. Furthermore, both *fBMVEC*s and *aBMVEC*s are essentially equally comparable as tested above.

To further characterize our *fBMVEC*s, we examined protein expression compared to *aBMVEC*s. Cells were lysed and proteins were separated by SDS-PAGE. Membranes were then probed for TJPs (ZO-1, occludin, claudin-5), transporters (Glut-1, MRP-5), the endothelial marker PECAM-1, and transferrin receptor (TfR) (Figure 3(a)). Western blots for two representative donors are shown which have no differences in protein expression of ZO-1, occludin, GLUT-1, and PECAM-1. MRP-5, TfR and claudin-5 expression was slightly different although not significantly between fetal and adult donors (Figure 3(b)). Additionally, immunofluorescence staining of the TJPs occludin (Figure 3(c)) and ZO-1 (supplemental Figure 3) showed the traditional BBB pattern that was distinctly localized only at the cell borders and was not different between *fBMVEC*s and *aBMVEC*s (Figure 3(c)). Overall, protein expression levels were comparable for many proteins, further supporting the similarities between isolated *fBMVEC*s and *aBMVEC*s.

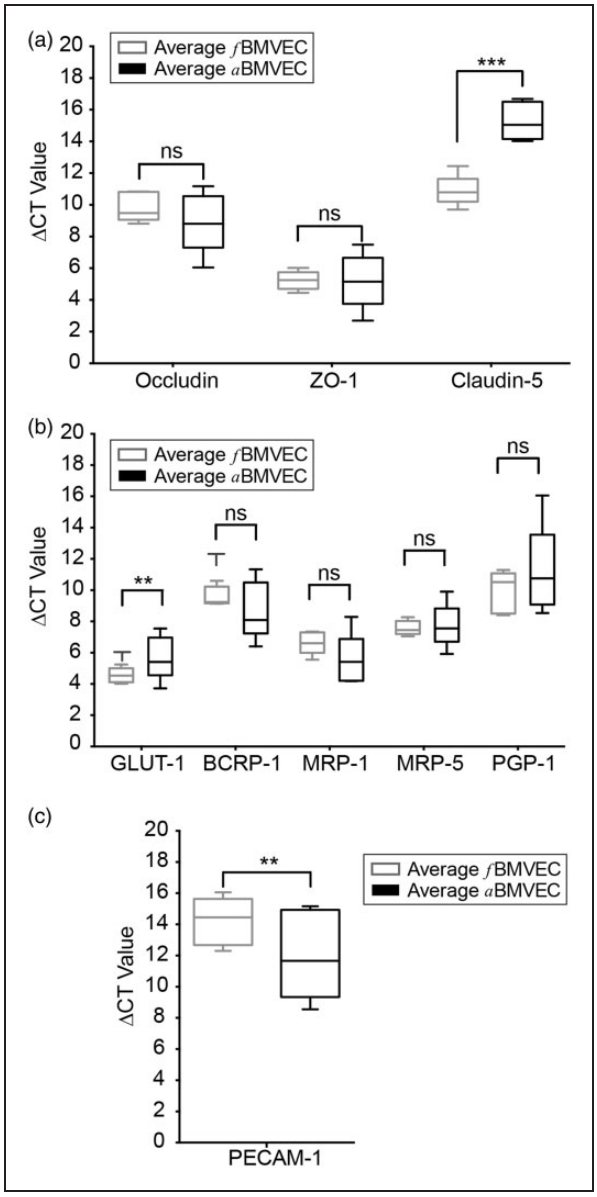

Figure 2. mRNA expression of tight junction proteins, adhesion molecules, and transporters in fetal and adult brain microvascular endothelial cells (BMVECs). mRNA from five *f*BMVEC and five *a*BMVEC donors was analyzed for gene expression of tight junction proteins (occludin, ZO-1, claudin-5), transporters (GLUT-1, BCRP-1, MRP-1, MRP-5, PGP-1) and a ubiquitous endothelial adhesion molecule (PECAM-1). Box and whisker plots are shown ofΔCT values for occludin and ZO-1 (a), BCRP-1, MRP-1, MRP-5, and PGP-1 (b), which were all non-significant between *f*BMVEC and *a*BMVEC donors. Fetal donors expressed lower levels of Claudin-5 (a) and Glut-1 (b) and higher levels of PECAM-1 (c) when compared to adults. Student's t-test $^*p < 0.05$.

Functional characterization of fBMVECs

High electrical resistance is a defining characteristic of the BBB and is commonly used to evaluate endothelial barrier integrity.[2] For the measurement of TEER, cells are grown on electrodes, and the small current applied travels between the cells and the resulting resistance measurements reflect the barrier properties of the monolayer. Thus, higher resistance means a "tighter" barrier. *fBMVEC*s and *aBMVEC*s were cultured in 96-well plates (Applied Biophysics) to measure the resistance of the monolayer in response to stimulus. To demonstrate the unique barrier properties of brain ECs, resistance measurements were obtained from four cell types: *fBMVEC*s, *aBMVEC*s, human coronary artery endothelial cells (HCAECs) and Human embryonic kidney cells 293 (HEKs). After three to five days, the media was exchanged and representative traces for the following 24 h (normalized to HEK absolute resistance values) were plotted (Figure 4). Non-barrier ECs displayed ~10-fold tighter monolayers and barrier-forming ECs (fetal and adult) displayed ~50-fold tighter monolayers than HEK cells.

To further investigate the functional aspects of the *fBMVEC*s barrier, we examined the response to a known barrier tightening agent, dexamethasone,[22] and disrupting agent, IL-1β.[23] Mixed fetal cultures, which do not form a continuous monolayer due to the lack of TJP complex formation between astrocytes/pericytes and BMVECs, were used to demonstrate the unique response of pure endothelial monolayers. *aBMVEC*s responded to dexamethasone with an 8% increase in resistance, while IL-1β decreased resistance by 26% (Figure 4(b)). *fBMVEC* TEER responded to dexamethasone and IL-1β similarly (increasing 8% and decreasing 17%, respectively) (Figure 4(c)). Conversely, mixed fetal cultures did not respond to dexamethasone and IL-1β with changes in TEER value of less than 10% (Figure 4(d)).

Another defining characteristic of a functional BBB is the upregulation of adhesion molecules, which initiates the adhesion and migration of monocytes through the endothelium.[18] Surface expression of ICAM-1 and VCAM-1 was characterized following endothelial activation with TNF-α (Figure 5). Basal expression of ICAM-1 averaged a mean fluorescence intensity of 377 ± 224 for *fBMVECs* and was not statistically different from *aBMVEC*s (data not shown). Flow cytometric analysis showed a time-dependent increase in of ICAM-1 and VCAM-1 surface expression, which became elevated at 6 h and was sustained through 48 h (Figure 5). All time points were significantly elevated compared to time 0, and the difference in magnitude of the adhesion molecule (ICAM-1, VCAM-1) upregulation was not statistically significant between *fBMVEC*s and *aBMVEC*s. In addition, adhesion and migration assays were performed as described previously[16–18] to demonstrate the functional response of the endothelium during inflammation. *fBMVEC*s

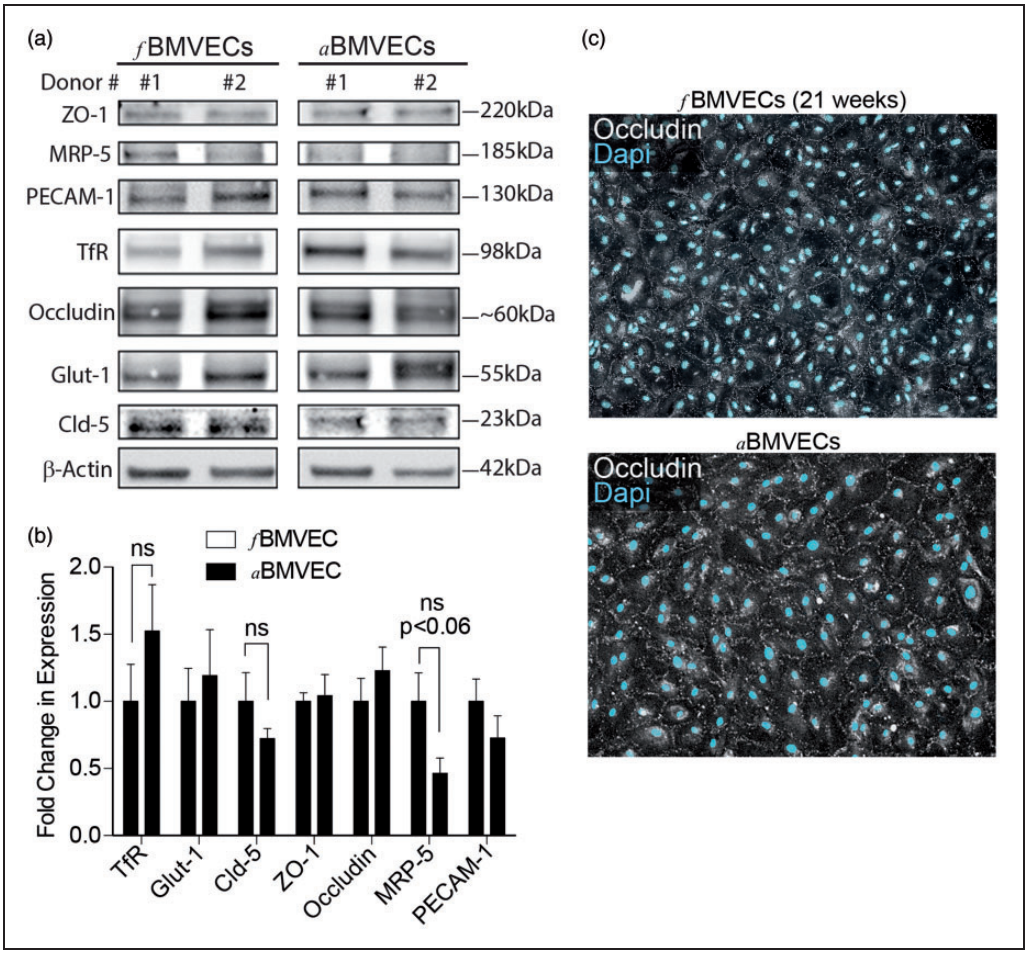

Figure 3. Protein expression analysis and immunofluorescence staining of *fBMVECs*. (a) Cell lysates for fetal and adult donors separated by SDS-page and probed for zona occludens-1 (ZO-1), multidrug resistance-associated protein-5 (MRP-5), platelet endothelial cell adhesion molecule-1 (PECAM-1), transferrin receptor (TfR), occludin, glucose transporter-1 (Glut-1), claudin-5, and β-Actin. Representative images for two fetal and two adult donors are shown. (b) Bar graph densitometry quantification showing non-significant differences in expression levels between fetal donors and adult donors. (c) Immunofluorescence staining of TJP occludin expression (white) in *fBMVECs* (top) and aBMVECs (bottom) showing occludin localization at cell boundaries (Dapi, Cyan). 10 × images. Scale bars 50 μm.

activated with TNF-α had ~2.5 × the number of adhered monocytes as compared to untreated cells (Figure 6(a)). Additionally, monocyte chemoattractant protein-1 (MCP-1) induced ~2 × more monocytes to migrate through the endothelium as compared to untreated cells (Figure 6(b) and (c)). Overall, these results demonstrate the response of *fBMVEC*s to inflammatory cytokines (TNF-α, IL-1β) through upregulation of adhesion molecules and that *fBMVEC*s exhibit the anticipated barrier response regarding adhesion and migration of monocytes.

An additional aspect to the use of human fetal tissue for BBB models is the potential for the development of syngenic tri-culture models derived from the same host. We have therefore provided a proof of concept BBB model using ECs, astrocytes, and pericytes derived from the same host grown in commercially available microfluidic chips (Figure 7(a) to (d)). Synvivo® microfluidic chips consist of two compartments separated by 10 μm "column-matrix."[24] The outer compartment, designed for ECs under fluidic flow, has a narrow height (100 μm) and width, while the inner CNS compartment has space for the growth of multiple cell types. Astrocytes and pericytes were obtained during the sorting process by selection of an ICAM-1 negative population. ECs were then plated in the EC compartment and grown to confluency. Fluorescently labeled astrocytes and pericytes were then plated in the CNS compartment (Figure 7(a) to (d)). In some areas, fluorescently labeled cells span the "column-matrix" connecting the CNS to the EC compartment (Figure 7(d), inset). We also provide brightfield

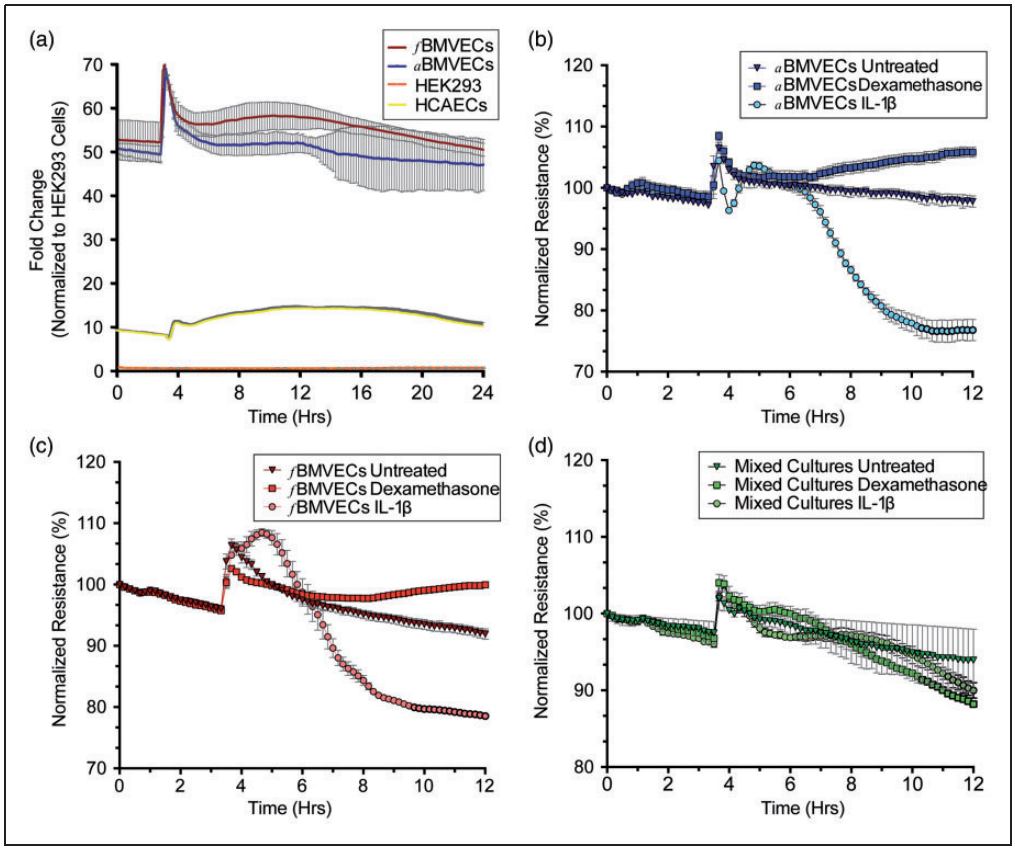

Figure 4. Evaluation of barrier trans-endothelial electrical resistance (TEER) for *fBMVECs* and *aBMVECs*. (a) *fBMVECs*, *aBMVECs*, human coronary artery endothelial cells (HCAECs) and human embryonic kidney cells 293 (HEK293) were grown on electrodes, and resistance (Ohms) was measured over time. After three to five days, the media was exchanged and representative traces for the following 24 h (normalized to HEK absolute resistance values) are shown. Non-barrier forming ECs are ~10-fold tighter than HEK cells, and barrier-forming ECs (fetal and adult) are ~50-fold tighter than HEK cells. (b) to (d). *fBMVECs* (b), *aBMVECs* (c), and mixed cultures (d) were challenged with barrier tightening (dexamethasone) and disrupting (IL-1β) agents. Pure barrier ECs (b & c) demonstrate changes in resistance in response to barrier tightening and disrupting agents in contrast to impure EC monolayers which fail to form tight barriers. TEER values are represented as the average (line) normalized TEER ± SEM (b) to (d).

images of the microfluidic chip at 4 × and 10 × with a mixed neuronal-glial-pericyte culture in the "CNS compartment" (Figure 7(g) and (h)). To demonstrate EC barrier integrity, fluorescently labeled tracers (NaFluo, 3 kDa CB-Dex and 40 kDa TMR-Dex) were perfused in the endothelial compartment and the fluorescently labeled dextrans can be seen confined to this outer compartment (Figure 7(i) and (j)). Stimulation with LPS statistically increased permeability as expected (Figure 7(i) and (j)). These studies, to assess the EC permeability, utilized this neuronal–glial–pericyte mixture in the CNS compartment.

Microfluidic devices also offer the ability to apply fluidic flow to ECs and recreate their in vivo environment. It has been well documented that upon isolation, ECs develop a cobblestone-like morphology, which is different from their in vivo phenotype. The in vivo phenotype is a result of the endothelial response to blood flow, which induces cytoskeletal rearrangement and alignment in the direction of the fluid flow.[25] To demonstrate the specific endothelial response to fluidic forces, *fBMVECs* were grown in microfluidic devices and subjected to fluidic flow for five days. Cells were then imaged using brightfield microscopy. *fBMVECs* responded to prolonged fluidic flow by aligning in the direction of fluid flow (Figure 7(f)). Overall, these results demonstrate the application of use *fBMVECs* in syngenic BBB models and that *fBMVECs* exhibit the expected response to fluidic flow involving morphological changes though cytoskeletal rearrangement to align in the direction of the flow.

Discussion

Human brain ECs are in high demand for the potential use in studying human disease pathology, screening of therapeutic agents, toxicity studies, and drug delivery. ECs are isolated from many vascular lineages although

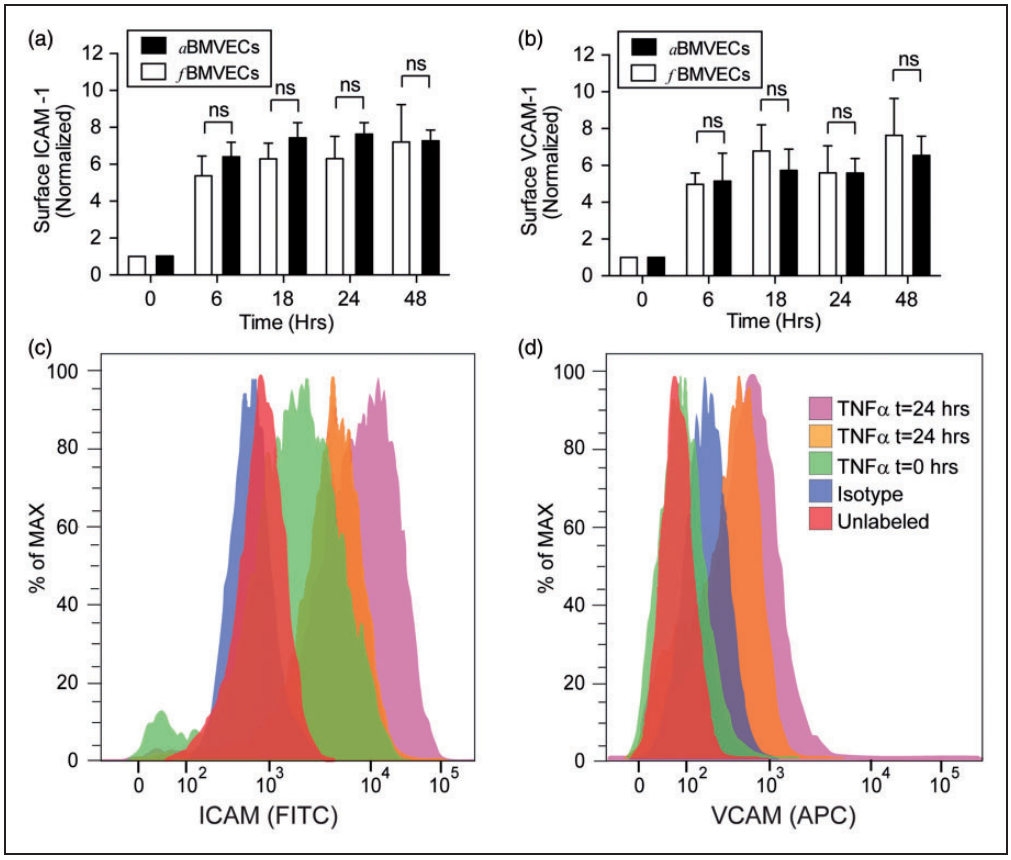

Figure 5. TNF-α induces upregulation of adhesion molecule expression in *fBMVECs*. Fetal and adult BMVECs were stimulated with TNF-α (100 ng/mL), harvested at 0, 6, 18, 24, 48 h and analyzed by flow cytometry. Bar graph and histograms show the upregulation of adhesion molecules ICAM-1 (a,c) and VCAM-1 (b,d) in response to TNF-α which was not statistically significant between *fBMVECs* and *aBMVECs*.

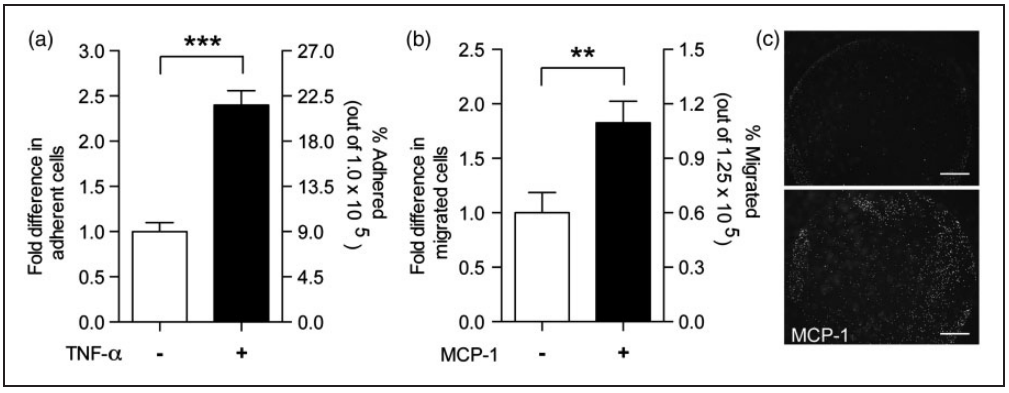

Figure 6. Functional assays of immune–endothelial interactions using *fBMVECs*. (a) Adhesion assay: *fBMVECs* were treated with TNF-α (20 ng/mL) for 18 h. Treatments were removed prior to addition of monocytes. Data are represented as fold difference (mean ± SEM) of adherent cells. Results show a 2.5-fold increased in adherent monocytes on activated as compared to unactivated ECs. (b) Trans-endothelial migration assay: Monocytes were added to the upper chamber of Transwell® membranes and allowed to migrate through *fBMVECs* towards MCP-1 in the lower chamber. Data are represented as fold difference (mean ± SEM) of migrated cells. Results show a ~2-fold increase in migrated monocytes with the addition of MCP-1. (c) Representative images of the underside of the Transwell® showing migrated Calcein-AM labeled monocytes with or without MCP-1 in the lower chamber. Scare bars 100 μm.

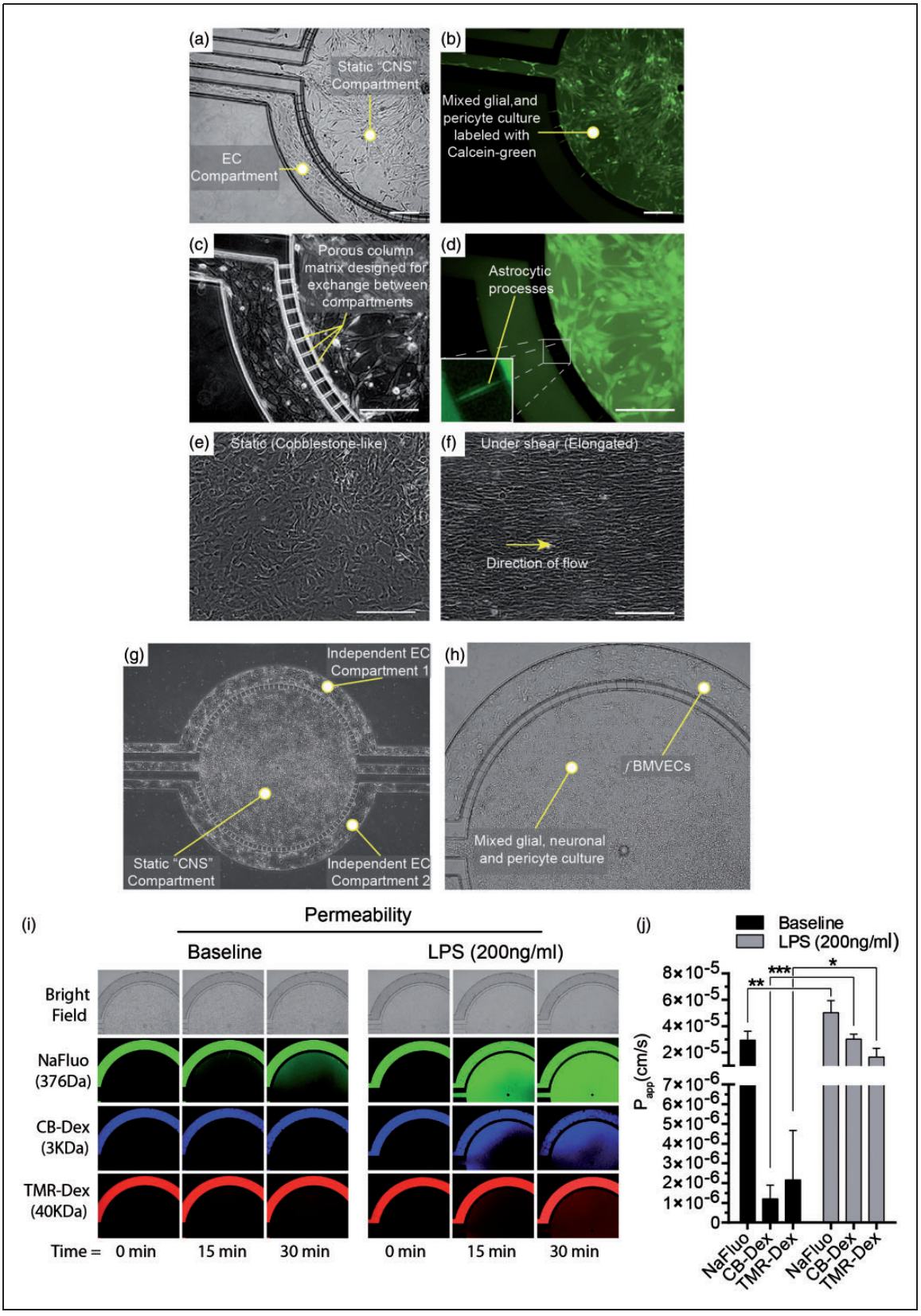

Figure 7. Proof-of-concept syngenic BBB model in a microfluidic chip using *fBMVECs*, astrocytes and pericytes derived from the same host. (a) and (c). Bright field images of *fBMVECs* grown in an outer endothelial compartment and an astrocyte/pericyte mixed culture in a separate inner "CNS compartment". (b) and (d). Astrocyte/pericyte cultures were labeled with Calcein-AM and then seeded into the "CNS compartment". Yellow arrowheads indicate areas where astrocytes span the column-matrix to connect with the endothelial compartment (d, insert). (e) and (f). *fBMVECs* align in the direction of fluid flow in microfluidic chambers.

(continued)

primarily from larger vessels (aorta, large veins) due to the ease in isolation, quantity, and availability. Microvascular ECs from specialized vasculature such as the brain have unique protein and gene expression profiles and functional properties, which make the use of alternative ECs lineages inadequate for modeling the BBB.[26] Additionally, while human ECs have become widely available by commercial sources, primary human brain ECs are an exception due to the limited availability of human brain tissue. Many labs without access to human tissue use other host species such as cow, pig, rat or mouse.[11] Alternatively, human immortalized brain EC lines are also available.[27] However, immortalized cell lines have a transformed phenotype, exhibit reduced barrier tightness, uncharacteristic expression patterns of TJPs, and overgrow instead of contact inhibit.[28,29] Tissue resected from epileptic patients is also a source of primary human BMVECs, for which our group has used extensively and published on how to isolate and culture successfully.[15] Unfortunately, only a few laboratories have access to resected tissue and alternative treatment options for epilepsy (such as radiosurgery) are now being favored over the open surgery procedure. Human fetal tissue offers a plausible alternative source of brain microvascular ECs from multiple donors and the opportunity to create syngenic tri-cultures using cells from the same host. However, previous attempts enabled fetal brain EC culture with only marginal to no barrier maturity. Furthermore, claims in the literature of brain EC (from human fetal tissue) for BBB modeling has not shown hallmark biochemical or functional BBB characteristics.[14,30] Here, we demonstrate that *fBMVEC*s isolated post-barrier development maintain suitable BBB properties for the use in in vitro BBB syngenic models.

Brain endothelium is highly specialized and performs vital functions in regulating the entry of molecules into the brain. These functions arise from the formation of TJs, which form a physical barrier, and the activities of metabolic transporters and enzymes at the BBB.[2] In addition, the means of evaluating these properties are well established. The physical barrier and regulation of paracellular permeability are developed by the expression pattern of TJPs such as occludin, claudin-5, ZO-1, and tricellulin.[2] Mature endothelium is evidenced in human fetal vessels by the localization of TJPs (occludin, claudin-5, tricellulin, and ZO-1) distinctly at the cell borders (Figure 1). Virgintino et al.[4] showed that in the developing human fetus, occludin and claudin-5 show a diffuse staining pattern prior to 14 weeks' gestational age,[4] which is consistent with our staining of 7- and 12-week-old vessels (Figure 1(a)). Interestingly, the TJPs ZO-1 and tricellulin have a different staining pattern over time in human fetal vessels compared to occludin and claudin-5 (Figure 1(a)). ZO-1 and tricellulin exhibit a junctional pattern as early as seven weeks, which is maintained at later gestational ages, compared to occluding and claudin-5 which show a transition from diffuse to junctional that is gestational age dependent (Figure 1). This difference highlights the importance of occludin and claudin-5 in mature barrier development and function. Following isolation, *fBMVEC*s continued to demonstrate this distinct junctional TJP expression pattern (Figure 3).

Comparison of *fBMVEC*s with *aBMVEC*s showed similarities in TJP mRNA (Figure 2(a)) and protein expression (Figure 3(a) and (b)). Few genes (Claudin-5, Glut-1 and PECAM-1) had different mRNA levels between *fBMVEC*s as compared to *aBMVEC*s, but protein expression was not different for PECAM-1 and Glut-1 (Figures 2 and 3). Claudin-5 expression was lower in *aBMVEC*s although not significantly, and this did not translate to a difference in functional barrier properties (Figure 4). MRP-5 was shown to have no difference in mRNA levels (Figure 2(b)) but expression varied in the *aBMVEC*s with a trend toward significantly higher expression in *fBMVEC*s by Western blot quantification (Figure 3). MRP-5 is highly expressed in human brain tissue[31] and studies indicate that transporter activity may be higher during development than in the adult,[21] which could explain the differences seen.

The formation of TJ complexes between ECs results in reduced paracellular permeability, which can be quantified by applying a current and measuring the resistance between cell-cell junctions.[16,18,23] Our results clearly show this as a unique aspect of barrier-forming endothelial monolayers as compared to non-barrier

Figure 7. Continued

Representative images of *fBMVEC*s before (e) and after (f) exposure to shear stress (10 dyn/cm^2). Yellow arrow indicates the direction of the fluid flow. Scale bars at 100 μm. (g) Bright field image (4×) of the microfluidic chip showing a mixed neuronal-glial-pericyte culture in the "CNS compartment" and *fBMVEC*s in the outer endothelial compartment. (h) Bright field close-up of (g). (10×). (i) Permeability of *fBMVEC*s during baseline and LPS insult. Fluorescently labeled tracers (sodium fluorescein, NaFluo, 3 kDa cascade blue dextran, CB-Dex and 40 kDa tetramethyrhodamine dextran, TMR-Dex) were perfused in the endothelial compartment to measure apparent permeability. The "CNS compartment" for the permeability studies include the neuronal–glial–pericyte mixture shown in (g) and (h). (i) Representative images for brightfield, NaFluo, CB-Dex, and TMR-Dex showing baseline and LPS stimulation (200 ng/mL) at time points 0, 15 min, and 30 min. (j) Bar graph quantification of the apparent permeability (P_{app}) for baseline and LPS insult (Avg ± SEM; *$p < 0.05$, **$p < 0.01$, ***$p < 0.001$).

ECs and HEK293 cells, which do not develop tight barriers (Figure 4(a)). Additionally, barrier tightening and disrupting agents induced changes in resistance due to a strengthening or dissolving of the TJ complex and was similar between our *fBMVEC*s and *aBMVEC*s (Figure 4(b) and (c)). Our results showed no significant differences between *fBMVEC*s and *aBMVEC*s (Figure 4(a)). Comparisons of our *fBMVEC*s and *aBMVEC*s with commercially available adult BMVECs (such as from Cell Systems Inc., ACBRI 376) would likely show a 10–20% difference (known from previous empirical findings) in tightness due to hydrocortisone, a known barrier-tightening agent (see the review by Benson et al.[32]) in the proprietary medium. Thus, a comparison with our cells would likely display an artificial difference in barrier tightness. In our efforts to compare *fBMVEC*s before and after barrier maturity, we found that isolation of *fBMVEC*s<14 weeks was exceptionally challenging. Of the few samples we received, we found that the ECs rapidly dedifferentiated or failed to proliferate after a couple of passages and early attempts to increase purity resulted in increased pericyte/smooth muscle cell contamination.

Aside from the functional aspect of regulating diffusion into the brain, ECs are known for their gate-keeping and recruitment properties regarding the immune system. In response to inflammatory cytokines, ECs upregulate adhesion molecules, which facilitate the adhesion and subsequent migration of monocytes.[2] As expected, TNF-α induced a time-dependent upregulation of ICAM-1 and VCAM-1 in both *fBMVEC*s and *aBMVEC*s (Figure 5). The magnitude of upregulation was not statistically different between the *fBMVEC*s and *aBMVEC*s demonstrating the intact functional nature of the EC response. Additionally, monocytes adhered and migrated through an intact BBB (Figure 6) similarly to previous studies with *aBMVEC*s.[16,33,34]

In terms of BBB models, co-culture microfluidic chips are an advanced model allowing for the recreation of 3D architecture and mechanical forces (fluid flow). The inclusion of these important aspects (interactions between multiple cell types and fluidic forces) more closely mimics the in vivo environment and has been shown to regulate BBB properties.[35–38] The use of human fetal tissue for BBB models also offers an additional benefit in the potential to develop syngenic human tri-culture models derived from the same host. A proof-of-concept syngenic model of *fBMVEC*s, astrocytes, and pericytes derived from the same host is provided (Figure 7(a) and (d)). Aside from the syngenic aspect to this model, the microfluidic chips allow for inclusion of cell–cell interactions through the ability of CNS cells to extend into the ''column-matrix'' to make connections with the ECs (Figure 7(d), inset). It was also demonstrated that the *fBMVEC*s formed a fully functional barrier as assessed by the restriction of fluorescently labeled tracers (NaFluo, 3 kDa CB-Dex, 40 kDa TMR-Dex) in the EC compartment (Figure 7(i) and (j)). Additionally, LPS insult increased the apparent permeability as expected (Figure 7(i) and (j)). The apparent baseline permeability for *fBMVEC*s is comparable to a recent study using *aBMVEC*s in a microfluidic model.[39] Overall, the use of the combined *fBMVEC*s and same donor fetal-derived cells in microfluidic chips provides the important structural and environmental factors needed to more accurately model an in vivo BBB.

Another unique aspect of endothelial biology is the response to the mechanical forces caused by fluid flow. The fluid creates a drag force or shear stress at the cell surface, which initiates a series of signaling pathways leading to cytoskeletal rearrangement.[25,29,40] ECs in the absence of fluid forces lose their in vivo phenotype and develop a cobblestone-like morphology. Upon exposure to uniform laminar shear stress, ECs undergo cytoskeletal rearrangement to develop an elongated spindle-shape, which aligns in the direction of the fluidic flow. The time for transition is dependent on the shear stress magnitude, host species, cell passage and potentially the time since isolation.[29] Recent studies on an immortalized human brain EC line have shown that these cells do not experience a morphological change in response to fluid flow[29,41] which was suggested as a unique response of brain microvascular ECs. However, our experience with primary human *fBMVEC*s and *aBMVEC*s leads us to believe that transformation into an immortalized cell line may alter or prevent the initiation of mechanotransduction and explain the differences in our results (Figure 7(f)).

We have demonstrated that *fBMVEC*s and *aBMVEC*s have similar mRNA, protein expression, barrier functions, and adhesion molecule upregulation. While some differences were detected in mRNA and protein expression, the functional aspects were not different validating *fBMVEC*s as an alternative model for BBB modeling. *fBMVEC*s also functioned similarly to *aBMVEC*s in traditional adhesion and migration assays demonstrating their intact functional properties. Additionally, we show the potential to develop human syngenic BBB models in microfluidic chips, which provide important aspects of the in vivo environment critical to the development of the BBB. Overall, this work demonstrates the ability to create BBB models from human fetal tissue, a valuable alternative BMVEC source, and their use has the potential to make significant advancements in our understanding of BBB physiology and the development of testing platforms that closely embodies the human BBB in vitro.

Funding

The author(s) disclosed receipt of the following financial support for the research, authorship, and/or publication of this article: This study was supported (in part) by research funding from the NIH: NIH-NINDS 1R01NS086570 (SHR), Shriners Hospitals for Children: 85110-PHI-14 (SHR), NIH-NIDA T32DA007237 (AMA, LAC) and F32DA041282 (AMA). The Laboratory of Developmental Biology was supported by NIH Award Number 5R24HD000836 from the Eunice Kennedy Shriver National Institute of Child Health & Human Development.

Acknowledgements

We would like to thank Dr. Michael Autieri for the gift of HCAECs and Dr. Xiaoxuan Fan from the Flow Cytometry Core at the Lewis Katz School of Medicine at Temple University for his assistance in cell sorting.

Declaration of conflicting interests

The author(s) declared no potential conflicts of interest with respect to the research, authorship, and/or publication of this article.

Authors' contributions

AMA and SHR contributed to the study design. AMA, EML, LAC, RR, MJS, SJK, NR conducted the experiments. AMA, SHR, EML, LAC, SFM, RR contributed to the writing of the manuscript. YP and DL contributed reagents.

Supplementary material

Supplementary material for this paper can be found at the journal website: http://journals.sagepub.com/home/jcb

References

1. Garlanda C and Dejana E. Heterogeneity of endothelial cells. Specific markers. *Arterioscler Thromb Vasc Biol* 1997; 17: 1193–1202.
2. Persidsky Y, Ramirez SH, Haorah J, et al. Blood-brain barrier: structural components and function under physiologic and pathologic conditions. *J Neuroimmune Pharmacol* 2006; 1: 223–236.
3. Cornford EM and Hyman S. Localization of brain endothelial luminal and abluminal transporters with immunogold electron microscopy. *NeuroRx* 2005; 2: 27–43.
4. Virgintino D, Errede M, Robertson D, et al. Immunolocalization of tight junction proteins in the adult and developing human brain. *Histochem Cell Biol* 2004; 122: 51–59.
5. Anstrom JA, Thore CR, Moody DM, et al. Immunolocalization of tight junction proteins in blood vessels in human germinal matrix and cortex. *Histochem Cell Biol* 2007; 127: 205–213.
6. Ballabh P, Hu F, Kumarasiri M, et al. Development of tight junction molecules in blood vessels of germinal matrix, cerebral cortex, and white matter. *Pediatr Res* 2005; 58: 791–798.
7. Wolburg H and Lippoldt A. Tight junctions of the blood-brain barrier: development, composition and regulation. *Vascul Pharmacol* 2002; 38: 323–337.
8. Licht T, Dor-Wollman T, Ben-Zvi A, et al. Vessel maturation schedule determines vulnerability to neuronal injuries of prematurity. *J Clin Invest* 2015; 125: 1319–1328.
9. Ribatti D, Nico B, Crivellato E, et al. Development of the blood-brain barrier: a historical point of view. *Anat Rec B New Anat* 2006; 289: 3–8.
10. Joo F and Karnushina I. A procedure for the isolation of capillaries from rat brain. *Cytobios* 1973; 8: 41–48.
11. Warren MS, Zerangue N, Woodford K, et al. Comparative gene expression profiles of ABC transporters in brain microvessel endothelial cells and brain in five species including human. *Pharmacol Res* 2009; 59: 404–413.
12. Mkrtchyan H, Scheler S, Klein I, et al. Molecular cytogenetic characterization of the human cerebral microvessel endothelial cell line hCMEC/D3. *Cytogenet Genome Res* 2009; 126: 313–317.
13. Barbaro NM, Quigg M, Broshek DK, et al. A multicenter, prospective pilot study of gamma knife radiosurgery for mesial temporal lobe epilepsy: seizure response, adverse events, and verbal memory. *Ann Neurol* 2009; 65: 167–175.
14. Navone SE, Marfia G, Invernici G, et al. Isolation and expansion of human and mouse brain microvascular endothelial cells. *Nat Protoc* 2013; 8: 1680–1693.
15. Bernas MJ, Cardoso FL, Daley SK, et al. Establishment of primary cultures of human brain microvascular endothelial cells to provide an in vitro cellular model of the blood-brain barrier. *Nat Protoc* 2010; 5: 1265–1272.
16. Rom S, Fan S, Reichenbach N, et al. Glycogen synthase kinase 3beta inhibition prevents monocyte migration across brain endothelial cells via Rac1-GTPase suppression and down-regulation of active integrin conformation. *Am J Pathol* 2012; 181: 1414–1425.
17. Rom S, Zuluaga-Ramirez V, Dykstra H, et al. Selective activation of cannabinoid receptor 2 in leukocytes suppresses their engagement of the brain endothelium and protects the blood-brain barrier. *Am J Pathol* 2013; 183: 1548–1558.
18. Rom S, Zuluaga-Ramirez V, Dykstra H, et al. Poly(ADP-ribose) polymerase-1 inhibition in brain endothelium protects the blood-brain barrier under physiologic and neuroinflammatory conditions. *J Cereb Blood Flow Metab* 2015; 35: 28–36.
19. Terrell-Hall TB, Ammer AG, Griffith JI, et al. Permeability across a novel microfluidic blood-tumor barrier model. *Fluids Barriers CNS* 2017; 14: 3.
20. Nagy Z, Peters H and Huttner I. Fracture faces of cell junctions in cerebral endothelium during normal and hyperosmotic conditions. *Lab Invest* 1984; 50: 313–322.
21. Saunders NR, Liddelow SA and Dziegielewska KM. Barrier mechanisms in the developing brain. *Front Pharmacol* 2012; 3: 46.
22. Romero IA, Radewicz K, Jubin E, et al. Changes in cytoskeletal and tight junctional proteins correlate with decreased permeability induced by dexamethasone in

cultured rat brain endothelial cells. *Neurosci Lett* 2003; 344: 112–116.
23. Wu L, Ramirez SH, Andrews AM, et al. Neuregulin1-beta decreases IL-1beta induced RhoA activation, myosin light chain phosphorylation, and endothelial hyper-permeability. *J Neurochem* 2016; 136: 250–257.
24. Deosarkar SP, Prabhakarpandian B, Wang B, et al. A novel dynamic neonatal blood-brain barrier on a chip. *PLoS One* 2015; 10: e0142725.
25. Vartanian KB, Berny MA, McCarty OJ, et al. Cytoskeletal structure regulates endothelial cell immunogenicity independent of fluid shear stress. *Am J Physiol Cell Physiol* 2010; 298: C333–C341.
26. Xiaozhuang Z, Xianqiong L, Jingbo J, et al. Isolation and characterization of fetus human retinal microvascular endothelial cells. *Ophthalmic Res* 2010; 44: 125–130.
27. Vu K, Weksler B, Romero I, et al. Immortalized human brain endothelial cell line HCMEC/D3 as a model of the blood-brain barrier facilitates in vitro studies of central nervous system infection by Cryptococcus neoformans. *Eukaryot Cell* 2009; 8: 1803–1807.
28. Weksler BB, Subileau EA, Perriere N, et al. Blood-brain barrier-specific properties of a human adult brain endothelial cell line. *FASEB J* 2005; 19: 1872–1874.
29. Reinitz A, DeStefano J, Ye M, et al. Human brain microvascular endothelial cells resist elongation due to shear stress. *Microvasc Res* 2015; 99: 8–18.
30. Navone SE, Marfia G, Nava S, et al. Human and mouse brain-derived endothelial cells require high levels of growth factors medium for their isolation, in vitro maintenance and survival. *Vasc Cell* 2013; 5: 10.
31. Dutheil F, Dauchy S, Diry M, et al. Xenobiotic-metabolizing enzymes and transporters in the normal human brain: regional and cellular mapping as a basis for putative roles in cerebral function. *Drug Metab Dispos* 2009; 37: 1528–1538.
32. Benson K, Cramer S and Galla HJ. Impedance-based cell monitoring: barrier properties and beyond. *Fluids Barriers CNS* 2013; 10: 5.
33. Ramirez SH, Fan S, Zhang M, et al. Inhibition of glycogen synthase kinase 3beta (GSK3beta) decreases inflammatory responses in brain endothelial cells. *Am J Pathol* 2010; 176: 881–892.
34. Ramirez SH, Hasko J, Skuba A, et al. Activation of cannabinoid receptor 2 attenuates leukocyte-endothelial cell interactions and blood-brain barrier dysfunction under inflammatory conditions. *J Neurosci* 2012; 32: 4004–4016.
35. Booth R and Kim H. Characterization of a microfluidic in vitro model of the blood-brain barrier (muBBB). *Lab Chip* 2012; 12: 1784–1792.
36. Cohen-Kashi Malina K, Cooper I and Teichberg VI. Closing the gap between the in-vivo and in-vitro blood-brain barrier tightness. *Brain Res* 2009; 1284: 12–21.
37. Siddharthan V, Kim YV, Liu S, et al. Human astrocytes/astrocyte-conditioned medium and shear stress enhance the barrier properties of human brain microvascular endothelial cells. *Brain Res* 2007; 1147: 39–50.
38. Gaillard PJ, Voorwinden LH, Nielsen JL, et al. Establishment and functional characterization of an in vitro model of the blood-brain barrier, comprising a co-culture of brain capillary endothelial cells and astrocytes. *Eur J Pharm Sci* 2001; 12: 215–222.
39. Herland A, van der Meer AD, FitzGerald EA, et al. distinct contributions of astrocytes and pericytes to neuroinflammation identified in a 3D human blood-brain barrier on a chip. *PLoS One* 2016; 11: e0150360.
40. Osborn EA, Rabodzey A, Dewey CF Jr, et al. Endothelial actin cytoskeleton remodeling during mechanostimulation with fluid shear stress. *Am J Physiol Cell Physiol* 2006; 290: C444–C452.
41. Ye M, Sanchez HM, Hultz M, et al. Brain microvascular endothelial cells resist elongation due to curvature and shear stress. *Sci Rep* 2014; 4: 4681.